Published in final edited form as:
Anal Biochem. 2010 June 1; 401(1): 154–161. doi:10.1016/j.ab.2010.02.023.

QUANTIFICATION OF CERAMIDE SPECIES IN BIOLOGICAL SAMPLES BY LIQUID CHROMATOGRAPHY-ELECTROSPRAY TANDEM MASS SPECTROMETRY

Takhar Kasumov[1,2,*], **Hazel Huang**[2], **Yoon-Mi Chung**[3], **Renliang Zhang**[4], **Arthur J. McCullough**[1,2], and **John P. Kirwan**[1,2]

[1] Department of Gastroenterology & Hepatology, Cleveland Clinic, Cleveland, OH

[2] Department of Pathobiology, Cleveland Clinic, Cleveland, OH

[3] Department of Cell Biology, Cleveland Clinic, Cleveland, OH

[4] Department of Research Core Services, Cleveland Clinic, Cleveland, OH

Abstract

We present an optimized and validated liquid chromatography-electrospray ionization tandem mass spectrometric (LC-ESI-MS/MS) method for the simultaneous measurement of concentrations of different ceramide species in biological samples. The method of analysis of tissue samples is based on Bligh and Dyer extraction, reverse-phase HPLC separation and multiple reaction monitoring of ceramides. Preparation of plasma samples also requires isolation of sphingolipids by silica gel column chromatography prior to LC-ESI-MS/MS analysis. The limits of detection and quantification are in a range of 5–50 pg/ml for distinct ceramides. The method was reliable for inter-assay and intra-assay precision, accuracy and linearity. Recovery of ceramide subspecies from human plasma, rat liver and muscle tissue were 78–91%, 70–99%, and 71–95%, respectively. The separation and quantification of several endogenous long-chain and very-long-chain ceramides using two non-physiological odd chain ceramide (C17 and C25) internal standards was achieved within a single 21 min chromatographic run. The technique was applied to quantify distinct ceramide species in different rat tissues (muscle, liver, and heart) and in human plasma. Using this analytical technique we demonstrated that a clinical exercise training intervention reduces the levels of ceramides in plasma of obese adults. This technique could be extended for quantification of other ceramides and sphyngolipids with no significant modification.

Keywords

sphingolipid; ceramide; lipidomics; insulin resistance; apoptosis; ESI-MS/MS

*Address for correspondence: Takhar Kasumov, PhD, Department of Gastroenterology & Hepatology and Pathobiology, Lerner Research Institute, Cleveland Clinic Foundation, 9500 Euclid Avenue/NE 4-206, Cleveland, OH 44195, Phone: 216 444 4189, kasumot@ccf.org.

C18, C24, C18:1 and C24:1 ceramides are designated for ceramides containing saturated and monounsaturated fatty acids, stearic, oleic and nervonic fatty acids, respectively.

Introduction

Ceramides play an important role in cell signaling, cell differentiation, proliferation and apoptosis, and are generated by *de novo* synthesis from palmitoyl-CoA and serine, and serve as a precursor for many sphingolipids [1]. As a secondary messenger in the sphingomyelin transmembrane signaling pathway, ceramides are also formed by the neutral Mg^{2+}-dependent sphingomyelynase catalyzed hydrolysis of spingomyelin in cell membranes [2]. Several other minor pathways [3], including hydrolysis of ceramide metabolites (galactosylceramide, glycosylceramide and ceramide 1-phosphate) and ceramidase-catalyzed acylation of sphingosine with distinct fatty acyl-CoAs also contribute to ceramide homeostasis [1].

Although it is not clear how the structure of individual ceramide species defines their physiological functions, it has been shown that ceramides containing specific fatty acids are generated in response to certain stimuli (tumor necrosis factor alfa or B-cell receptor induced apoptosis), underscoring the structure/function relationship for different ceramide species [4]. It is known that C16 and C24 ceramide species are involved in cell death [5,6], while C18 ceramide inhibits cell growth [7].

Recent interest in ceramides has increased due to their newly identified role in insulin resistance [8]. From *in vitro* studies, it is known that ceramides inhibit glucose uptake through inhibition of Akt, a serine protein kinase mediator of insulin action [9]. In addition, ceramide content is increased in muscle, liver and adipose tissue in insulin resistant animal models [10]. Elevated total ceramide levels in human muscle [11] and adipose tissue has been linked to peripheral insulin resistance [12]. Recently we demonstrated that plasma ceramides are increased in obese subjects with type 2 diabetes and are associated with reduced insulin sensitivity [13]. However, the definite intracellular origin and physiological significance of different species of plasma ceramides are unknown. Since, intracellular partitioning of fatty acids and their metabolites play a significant role in insulin resistance and lipotoxicity [14], it is important to identify the role of specific ceramides in these processes.

Investigation of the physiological function of distinct ceramides requires an accurate, precise and sensitive method for their quantification in plasma and tissue biopsy samples. Currently ceramides are analyzed by an enzymatic diacylglycerol (DAG) kinase assay [15], by thin-layer chromatography (TLC) detection [16], high performance liquid chromatography (HPLC) [17,18], and gas chromatography mass spectrometry (GC-MS) analysis after derivatization [19]. In some cases the TLC-isolated ceramides are hydrolyzed, and the released fatty acids and sphingosine are analyzed after derivitization by gas-liquid chromatography [20], or by HPLC [21]. However, these methods are cumbersome and time consuming. While some of these approaches may be used to analyze total ceramide, they do not provide data on individual ceramide species [15,21]. In addition, existing methods provide discrepant results for ceramide levels in different biological samples [22–24]. Recent developments in electrospray ionization tandem mass spectrometry (ESI-MS/MS) have helped resolve some of these limitations. Several lipidomic studies have used ESI-MS/MS technologies to analyze ceramides and related sphingolipids in biological samples [25,26]. However, in many instances, the described methods attempt wide range lipidomic analyses, that make the validation and optimization of measuring multiple individual anlytes difficult. Recently, an optimized and validated tandem mass spectrometry analysis of a single C18 ceramide in cell culture was reported [27]. As part of our research on lipid related mechanisms of insulin resistance, we have optimized and validated a reverse-phase liquid chromatography coupled ESI-MS/MS technique for the simultaneous measurement of multiple ceramide species in different biological matrices. We have verified this technique for ceramide profiling and quantification in healthy human plasma and different rat tissues. We also demonstrate that this technique detects changes in human plasma ceramide levels after a clinical exercise intervention. This technique may also be

extended for quantification of other ceramides and related sphingolipids without significant modification to the methodology.

Material and Methods

Materials

Pure standards of endogenous ceramide subspecies (C14, C16, C18, C18:1, C20, C24 and C24:1) and non-naturally occurring internal standards (C17 and C25 ceramides) were obtained from AVANTI Polar Lipids Inc. (Alabaster, AL, purity > 99%). HPLC grade solvents for ESI-MS/MS and lipid extraction were purchased from Fluka (Milwaukee, MO). All other chemicals, including Merck grade silica gel (9385, 230–400 mesh, 60 Å) were from Sigma-Aldrich (St. Louis, MO).

Standard solutions

The stock solutions of ceramides were prepared at 1 mg/ml in chloroform. After dilution with ethanol, a working solution of C14, C16, C18, C18:1, C20, C24 and C24:1 mixture was prepared at 714 ng/ml for each ceramide species in one solution. This solution was divided into 0.5 ml fractions and saved at (−80°C) until analysis. A mixture of C17 and C25 solution in ethanol at concentrations of 1000 ng/ml and 2000 ng/ml, respectively, was prepared as an internal standard solution. Fifty μl of internal standard solution corresponding to 50 ng of C17 and 100 ng of C25 was used for each analysis.

Analytical methods

Validation studies

Linearity: Calibration curves for measurement of ceramide concentrations were constructed in a 50 μl plasma matrix with different concentrations of each endogenous ceramide (0–178 ng/ml for C14, 0–357 ng/ml for C16, C18, C18:1 and C20 and 0–714 ng/ml for C24 and C24:1) in a mixed solution containing seven ceramide standards. These ranges cover all ceramide species found in biological fluids and tissues. All samples were spiked with constant amounts of C17 and C25 ceramide internal standards. Linear regression equations were derived from calibration curves, and were used to calculate ceramide concentrations in plasma and tissue samples. Analytical sensitivity was estimated from the calibration curve slopes. The limit of quantification (LOQ) was defined as the lowest point in the calibration curve with a signal/noise ratio equal to 10. The limit of detection was defined as a signal/noise ratio equal to 3.

Accuracy and Recovery

Accuracy and Recovery: ***Plasma Recovery:*** Three sets of samples were prepared for an accuracy and recovery study of ceramide concentrations. The first set of samples included 100 μl of a solution of different ceramides in ethanol at four different amounts: 5.6, 22.3, 44.5 and 178 ng for C14, C16, C18, C18:1 and C20, and 15.6, 31.3, 62.5 and 250 ng for C24 and C24:1. The second set of samples consisted of duplicates of 50 μl plasma samples. For the third set, samples with different amounts (same as in set 1) of ceramides were each spiked with 50 μl of plasma. All samples were spiked with C17 (50 ng) and C25 (100 ng) ceramides as internal standards. All plasma samples were aliquoted from the same pooled plasma. After quantification of individual ceramides in each sample, the recovery of the assay was calculated as the ratio of analyte (ceramide) concentration in spiked plasma to the sum of the non-spiked plasma and pure standards.

Tissue recovery: Recovery for the ceramide isolation from tissue was assessed using a ceramide standard mixture with and without powdered tissue homogenate (rat liver and muscle) in parallel with tissue samples, which were not spiked with ceramide standard mixture. All

samples were spiked with C17 and C25 internal standards. The recovery of ceramides from tissues was calculated using the same procedure as for recovery of ceramides from plasma. The precision, i.e., intra-assay and inter-assay reproducibility of the method was determined by multiple analyses of a plasma sample from pooled plasma. Intra-assay variability was determined by analyzing one sample five times. Inter-assay was established by processing the same sample in five different preparations on different days over 2 weeks.

Human Study—We investigated ceramide levels in five healthy adults who participated in our ongoing studies on the effect of exercise on insulin sensitivity. Subjects were obese but had normal glucose tolerance. All individuals gave their written informed consent to partake in the study, and all protocols were approved by the Institutional Review Board of the Cleveland Clinic. Plasma for ceramide analysis was obtained prior to and after a 12-week clinical exercise intervention. For the three days immediately prior to and during the last three days of the intervention, all subjects resided in our Clinical Research Unit. They were placed on isocaloric diets based on estimated basal metabolic rates to ensure weight stability prior to metabolic testing. Exercise was supervised and consisted of aerobic training for 1 hr/day, 5 d/wk at 80% of HR_{max} (~70% VO_{2max}). Fasting blood samples (1 ml, in EDTA coated tubes) were obtained from a dorsal hand vein before and after the intervention. Blood samples were centrifuged immediately at 4°C and the separated plasma was stored at (−80°C) until analysis.

Sample Preparation for Human Plasma Ceramide Analysis: Plasma samples were defrosted and 50 μl aliquots were transferred to ice-cold screw-capped glass tubes placed on ice. Samples, in parallel with standard solutions, were spiked with 50 ng of C17 and 100 ng of C25 ceramides and were extracted with 2 ml of a chloroform/methanol (1:2) mixture according to the protocol of Bligh and Dyer [28]. Phases were broken by adding 0.5 ml chloroform and 0.5 ml water. The lower organic fraction was removed and the remainder was extracted with an additional 1 ml of chloroform. The pooled organic phase was dried under nitrogen gas and the residue was reconstituted in 500 μl of methylene chloride and loaded onto a silica gel column packed with 2 ml of silica gel suspension in methylene chloride. Columns were washed with 1 ml of methylene chloride and ceramides were eluted with 2×2 ml of 30% isopropanol in methylene chloride. Eluent was dried under nitrogen gas and the residue was reconstituted in acetonitrile/2-propanol (60:40, v/v) containing 0.2% formic acid and analyzed by mass spectrometry.

Animal Study—All animal procedures were approved by the Institutional Animal Care and Use Committee (IACUC) at the Cleveland Clinic and were performed in accordance with NIH guidelines. Male Sprague-Dawley rats (200–300 g) were purchased from Charles River Laboratories (Wilmington, MA), and were housed in our animal care facility with a 12:12 h light-dark cycle. The animals had free access to food (Harlan Teklad NIH rat diet) and water. After three days of acclimation the animals were euthanized with sodium pentobarbital (120 mg/kg). The liver, heart and skeletal muscle were harvested rapidly and the tissues were continuously sprayed with ice-cold saline. Tissues were immediately freeze-clamped on aluminum blocks precooled in liquid nitrogen and saved at −80 °C until analysis.

Sample Preparation for Rat Tissue Ceramide Analysis: Frozen tissue samples were powdered under liquid nitrogen. For each analysis an aliquot of tissue powder (7–15 mg wet weight) was suspended in ice-cold saline solution (500 μl, 1M NaCl) and homogenized with a glass mortar and pestle. Calibration curves for ceramide standards using C17 and C25 ceramides as internal standards were prepared and processed in parallel with tissue samples. Ceramides from tissue homogenates were extracted using a similar protocol as for plasma. Briefly, 2 ml of an ice-cold chloroform: methanol (1:2, v/v) mixture was added to homogenized tissue and vortexed at 4°C. The pooled organic phase was filtered using a glass wool filter

packed in a pasteur pipette to remove any solid particles. Collected eluent was dried and the residue was reconstituted in HPLC elution buffer and analyzed by mass spectrometry. All ceramide measurement experiments were normalized for wet tissue weight.

High Performance Liquid Chromatography-Mass Spectrometry Analysis: Ceramide species were quantified by LC-ESI-MS/MS. For optimization, the mixture of ceramide standards was infused directly into the mass spectrometer and all source parameters and ionization conditions were adjusted to improve the sensitivity of the assay. Extracted samples (25 μl) were injected into a Waters HPLC (2690 Separation Module, Waters Corp., Milford, MA) and separated through an Xperchrom 100 C8 column (2.1 × 150 mm, 5 μm, P.J. Cobert Associates, St. Louis, MO). The ceramides were resolved using a gradient starting from 50% mobile phase A (water containing 0.2% formic acid) at a flow rate of 0.3 ml/min for 1 min, to 100% mobile phase B (acetonitrile/2-propanol (60:40, v/v) containing 0.2% formic acid) over 3 min at a linear gradient, and then with 100% B for 12 min. The column was then equilibrated for 5 min with 50% mobile phase B. The HPLC column effluent was introduced onto a Micromass triple quadrupole mass spectrometer (Quattro Ultima, Waters Inc., Beverly, MA) and analyzed using electrospray ionization in positive mode. The configurations for mass spectrometry were: capillary voltage, 3.0 kV; cone voltage, 40 V; source temperature, 120°C; and desolvation temperature, 250°C. The flow rate of the nitrogen gas in the cone and desolvation gas were 86 L/h and 700 L/h, respectively. Argon gas was used for collision-induced dissociation having the collision cell pressure at 8.43×10^{-4} mbar. Analyses were performed using electrospray ionization in the positive-ion mode with multiple reaction monitoring (MRM) to select both parent and characteristic daughter ions specific to each analyte simultaneously from a single injection. The MS/MS transitions (m/z) were 510→264 for C14, 538→264 for C16, 552→264 for C17, 564→264 for C18:1, 566→264 for C18, 594→264 for C20, 648→264 for C24:1, 650→264 for C24, and 664→264 for C25. The data were acquired using MassLynx software (version 4.1, Manchester, UK).

Quantification: Ceramide subspecies were quantified using calibration curves and the ratios of the integrated peak areas of ceramide subspecies and internal standards. C17 ceramide was used as an internal standard for quantification of C14, C16, C18, C18:1, and C20 subspecies. Concentrations of C24 and C24:1 were quantified using C25 as an internal standard. Total measured ceramide was calculated from the sum of C14, C16, C18:1, C18, C20, C24:1 and C24 ceramide subspecies.

Data are presented as mean ±SD. Paired t-tests were used to examine the effects of exercise on plasma ceramide levels. Significance was accepted when $P<0.05$.

Results

Tandem mass spectrometry optimization

The full scan MS/MS spectra were recorded in a positive-ion mode during direct infusion of ceramide standards. All of the investigated ceramide species give simple positive-ion full scan spectra in acetonitrile/2-propanol (60:40, v/v) containing 0.2% formic acid, confirming that at acidic pH in the ion spray ionization process, ions are mainly produced by protonation of neutral molecules ($M+H^+$) [29–31]. Precursor ions for each ceramide were separated and scanned in the first quadrupole (Q1), fragmented in the second quadrupole (Q2) and the product ions were scanned in the third quadrupole (Q3). Fig. 1 shows typical product ions spectra for some specific ceramide species. Consistent with the published literature [30,32], we found that collision-induced ionization of all studied ceramide species generates stable product ions with m/z 282 and 264 corresponding to the loss of an amide-bound acyl-group, and one or two molecules of water, respectively (Fig. 2). In addition, ceramides generate stable ions at a m/z

difference of 18, accounting for the loss of a water molecule from the precursor ion. Since m/z 264 is a high intensity ion, we optimized the electrospray parameters and collision energy to increase the intensity of each precursor ion in combination with m/z 264 in MRM mode for sensitive analysis of all species.

Liquid chromatography

Our orientation experiment with HPLC-MS/MS analysis of plasma and tissue samples after Bligh and Dyer lipid extraction without further purification revealed the existence of interfering peaks on HPLC chromatography and low sensitivity in mass spectrometry detection for plasma but not for tissue samples. Therefore we developed an easy-to-use silica chromatography approach for the isolation of sphingolipids from other abundant plasma lipids. This resulted in a significant improvement in the HPLC chromatography and yielded higher sensitivity in the plasma sample analysis. As a result, the chromatographic method proved suitable for separation of all analyzed ceramides within a single run on a C8 reverse-phase column using MS/MS detection. After testing different acidic organic eluent systems (pure and mixture of acetonitrile, methanol and isopropanol gradients with acidic water) we found that the mixture of acetonitrile/2-propanol (60:40, v/v) containing 0.2% formic acid gradient with acidic water allows separation of 9 ceramide species (7 physiological ceramides and 2 non-naturally occurring internal standards) on a C8 reverse-phase column in less than 5 min during a 21 min run; this includes column re-equilibrium (Fig. 3). Although the MRM mode with different transitions allows specific identification of coeluting ceramides, the chromatographic separation allows discrimination between ^{13}C isotope contributions from lower to higher molecular masses [31]. These results indicate that the chromatographic separation that we have described improves the specificity of the assay.

Assay validation—Calibration curves for a mixture of ceramide concentrations were made by adding increasing amounts of ceramides to constant amounts of C17 and C25 ceramide. The curves were linear over a range of 2.8–178 ng for C14, 2.8–357 ng for C16, C18, C18:1 and C20 ceramides, and 5.6–714 ng for C24 and C24:1 ceramides. The limit of detection, limit of quantification (LOQ) and linear regression parameters of calibration curves are presented in Table 1. These ranges cover all concentrations of ceramides found in human plasma and tissues.

Results from the accuracy study for the determination of C14, C16, C18:1, C18, C20, C24:1 and C24 concentrations are presented in Fig. 4. We plotted different concentrations of ceramide species that had been determined in plasma against the amount of these ceramides added to plasma. The resulting lines of identity were linear with slopes and regression coefficients close to 1. The *y* intercepts correspond to the plasma content of each ceramide, which is in good agreement with literature values [33]. Based on these analyses, the calculated percentage recoveries of different ceramide species from plasma were between 78±7% and 91±11% (Table 2). Intra-assay and inter-assay coefficient of variation for the assay were 0.2–3.3% and 0.2–7.3%, respectively (Table 3).

Likewise, as shown in Table 4 the recovery of ceramide species from rat liver and muscle tissue was relatively good (70–90%). The ceramide content determined in non-spiked tissue in this recovery study is in agreement with literature values [17,23], and is comparable with the liver and muscle ceramide levels determined from 5 different rats (Table 5).

After optimization and validation, we applied this technique to the determination of ceramide levels in human plasma and different rat tissues. Concentrations of C14, C16, C18:1, C18, C20, C24:1 and C24 ceramide species in plasma of healthy human adults before and after a twelve week clinical exercise intervention are presented in Table 6. The major ceramide species were C16, C24 and C24:1, corresponding to ~37%, ~28%, and ~9% of total measured ceramides.

The medium-chain C14 ceramide had the lowest concentration of the seven measured ceramide species (~5% of total measured ceramides). These values are similar to those found for plasma ceramides reported in previous publications [33,34].

Table 5 represents the results of our tissue analysis of the same ceramide species from 5 rats in comparison with literature values determined by different methods [17,23,35]. In agreement with the literature, our results show that ceramides containing palmitic and stearic acids (C16 and C18 ceramides) are the predominant ceramide species in rat myocardium. In contrast to a previous report [35], our results demonstrate that C20, C24 and C24:1 also have high abundance in rat heart.

Additionally, we found that the abundance of ceramides with C16, C24 and C24:1 fatty acids was also high in the liver, which is also in good agreement with literature values [23]. In contrast to rat myocardium, C18 ceramide only accounted for ~2% (~1.9 % in this study, compared to ~2.3 % in literature [23]) of total measured liver ceramides in the rat. Analysis in rat muscle tissue revealed high levels of long-chain and very-long-chain fatty acid containing ceramides. The content of C18 ceramide accounted for approximately one quarter of the total ceramides in muscle. With the exception of C14 ceramide (2.6±0.4 ng/g w.w.), all other measured ceramides accounted for substantial fractions of the total ceramide content. Thus, rat heart, liver, and muscle analysis, demonstrates that C16, C18, C20 and C24 are major saturated ceramides in all tissues. From two unsaturated ceramides measured in this study C24:1 is abundant in all three tissues, while C18:1 has higher abundance only in rat muscle.

Discussion

In this report we present an optimized and validated technique for the simultaneous quantification of a wide range of ceramide species in biological samples. Utilization of two non-physiological ceramides as internal standards (C17 and C25) allowed quantification of ceramides containing long-chain (C14, C16, C18, C18:1 and C20) and very-long-chain (C24:1 and C24) fatty acids in a single run. Analysis of the concentration profile of multiple ceramide species requires 50 μl of plasma or ~10 mg (wet weight) of tissue. Thus, the high sensitivity of this technique makes ceramide analysis possible, not only in biological fluids, but also in small size human tissue biopsy samples. The simultaneous measurement of ceramide species in plasma and different tissue samples will advance the investigation of the physiological significance of ceramides, and open the possibility that plasma ceramides can be used as biomarkers of insulin resistance, and/or apoptosis.

The wide concentration range of different ceramides in plasma and tissue (from nM to μM concentrations) requires a sensitive and versatile method for their analysis. Several HPLC [18], HPLC-MS [24,29,36] and gas GC-MS [19] approaches have been described for determining concentrations in biological samples. Although HPLC and GC-MS instruments are easily available and widely used for measuring ceramide concentrations, all of these techniques require derivatization prior to analysis. In contrast, HPLC-MS assays are more sensitive and do not require derivatization. This simplifies the assay and helps to avoid experimental errors generated at different levels of the analysis. Recent HPLC-MS based lipidomic and sphingolipidomic initiatives offer comprehensive profiling of multiple lipid compounds [25,26]. However, optimization of the absolute quantification of individual analytes has not yet been established. Since different lipids have distinct physicochemical properties, one of the major challenges in lipid analysis is the selection of an appropriate internal standard for quantification of individual analytes. Liebisch and colleagues used non-naturally occurring C8 ceramide as an internal standard for quantification of long-chain and very-long-chain ceramides using calibration lines constructed for a few ceramide species (C16, C18:1 and C24:1) [30]. These data were then used to calculate concentrations of the closest

related species. When these observations are combined with the results from our study (Table 1, column 5) it is evident that different ceramide species have different mass spectrometric ion responses. This necessitates the construction of individual calibration curves for each species. In addition, our initial analysis of pure ceramide standards revealed ion suppression at higher concentrations; this was substantial for C24 and C24:1 ceramides. When we used a C17 ceramide as a sole internal standard the result was distortion of the calibration lines toward an exponential curve for these specific species (data not presented). Therefore, we elected the C25 ceramide as the structurally-closest non-naturally occurring ceramide internal standard for the quantification of C24 and C24:1.

Another improvement in the ceramide analysis was achieved by purification of plasma ceramides on silica chromatography after total lipid extraction, prior to LC-MS/MS analysis. This step allows elution of sphingolipids in one fraction after washout of the most abundant and non-polar lipids, using methylene chloride. The result was good liquid chromatography separation and sensitive analysis of ceramide species in plasma. However, the lower lipid content of tissue samples allowed us to eliminate the silica column chromatography step.

The validation of this technique demonstrates that it is linear, accurate, precise, and free of any appreciable plasma and tissue matrix effect. The use of MRM mode based tandem mass spectrometry provides sufficient selectivity and sensitivity to the method. This easy-to-use analysis of ceramides bodes well for its routine application in basic and clinical translational research. The separation of several ceramide species by HPLC in a short single run (21 min for one sample analysis cycle) will allow this technique to be applied to high-throughput analysis.

After validation and optimization we applied this technique to the quantification of ceramide species in human plasma and rat tissues. The extracellular ceramide concentrations could be affected by Zn^{2+} dependent acidic spingomyelinase in blood and tissues [37]. If not stabilized, sphingomyelinase may generate ceramide from sphingomyelin in blood and tissue samples after collection. Therefore, in order to circumvent the post-collection ceramide metabolism, blood samples were collected in tubes containing ion chelating EDTA (in order to deactivate Zn^{2+} dependent acidic spingomyelinase), centrifuged immediately, and the plasma was stored at −80°C until analysis. It has been shown that fluorinated anesthetics (isoflurane and desflurane), but not pentobarbital stimulate renal cortical ceramide expression through the sphingomyelinase cascade [38]. Therefore, we used pentobarbital to anesthetize the rats. The high sensitivity of the method allowed us to assess the concentration profiles of multiple ceramide species in small sample volumes. The technique was verified by comparing our results for the different ceramide levels with values reported in the literature using different techniques. We also tested this assay by measuring changes in plasma ceramide levels in the same subjects before and after a clinical exercise intervention. The method enabled us to detect significant reductions in C14, C18:1, and C24 ceramide levels. Further, recent data on carbon tetrachloride- and lipolysaccharide-treated rats indirectly suggest that plasma ceramides originate from necrotized liver [23,24,39]. Establishing a direct link between plasma and hepatic ceramides in humans with liver disease may allow the use of plasma ceramides as biomarkers of hepatic dysfunction and cell death.

In conclusion, we have developed and validated an HPLC coupled tandem mass spectrometry analysis for the quantification of ceramide species in plasma and tissue samples. This technique could be used to study the regulation of ceramide homeostasis and its relation to diseases associated with altered lipid metabolism.

Acknowledgments

We thank Thomas Solomon for helpful discussions during preparation of the manuscript, and the CRU staff for their help with the human studies. This work was supported in part by National Institutes of Health grants RO1 AG12834, CTSA UL1-RR024989, and by the Cleveland Clinic Foundation.

Abbreviations used

ESI-MS/MS	electrospray ionization tandem mass spectrometry
MRM	multiple reaction monitoring
HPLC	high performance liquid chromatography
GC-MS	gas chromatography mass spectrometry
LOQ	limit of quantification

References

1. Huwiler A, Kolter T, Pfeilschifter J, Sandhoff K. Physiology and pathophysiology of sphingolipid metabolism and signaling. Biochim Biophys Acta 2000;1485:63–99. [PubMed: 10832090]
2. Clarke CJ, Snook CF, Tani M, Matmati N, Marchesini N, Hannun YA. The extended family of neutral sphingomyelinases. Biochemistry 2006;45:11247–11256. [PubMed: 16981685]
3. Ohanian J, Ohanian V. Sphingolipids in mammalian cell signalling. Cell Mol Life Sci 2001;58:2053–2068. [PubMed: 11814056]
4. Pewzner-Jung Y, Ben-Dor S, Futerman AH. When do Lasses (longevity assurance genes) become CerS (ceramide synthases)?: Insights into the regulation of ceramide synthesis. J Biol Chem 2006;281:25001–25005. [PubMed: 16793762]
5. Osawa Y, Uchinami H, Bielawski J, Schwabe RF, Hannun YA, Brenner DA. Roles for C16-ceramide and sphingosine 1-phosphate in regulating hepatocyte apoptosis in response to tumor necrosis factor-alpha. J Biol Chem 2005;280:27879–27887. [PubMed: 15946935]
6. Seumois G, Fillet M, Gillet L, Faccinetto C, Desmet C, Franđcois C, Dewals B, Oury C, Vanderplasschen A, Lekeux P, Bureau F. De novo C16- and C24-ceramide generation contributes to spontaneous neutrophil apoptosis. J Leukocyte Biol 2007;81:1477–1486. [PubMed: 17329567]
7. Koybasi S, Senkal CE, Sundararaj K, Spassieva S, Bielawski J, Osta W, Day TA, Jiang JC, Jazwinski SM, Hannun YA, Obeid LM, Ogretmen B. Defects in cell growth regulation by C18:0-ceramide and longevity assurance gene 1 in human head and neck squamous cell carcinomas. J Biol Chem 2004;279:44311–44319. [PubMed: 15317812]
8. Holland WL, Summers SA. Sphingolipids, insulin resistance, and metabolic disease: new insights from in vivo manipulation of sphingolipid metabolism. Endocrinol Rev 2008;29:381–402.
9. Pickersgill L, Litherland GJ, Greenberg AS, Walker M, Yeaman SJ. Key role for ceramides in mediating insulin resistance in human muscle cells. J Biol Chem 2007;282:12583–12589. [PubMed: 17337731]
10. Samad F, Hester KD, Yang G, Hannun YA, Bielawski J. Altered adipose and plasma sphingolipid metabolism in obesity: a potential mechanism for cardiovascular and metabolic risk. Diabetes 2006;55:2579–2587. [PubMed: 16936207]
11. Adams JM 2nd, Pratipanawatr T, Berria R, Wang E, DeFronzo RA, Sullards MC, Mandarino LJ. Ceramide content is increased in skeletal muscle from obese insulin-resistant humans. Diabetes 2004;53:25–31. [PubMed: 14693694]
12. Kolak M, Westerbacka J, Velagapudi VR, Weagsèater D, Yetukuri L, Makkonen J, Rissanen A, Heakkinen AM, Lindell M, Bergholm R, Hamsten A, Eriksson P, Fisher RM, Oresic M, Yki-Jearvinen H. Adipose tissue inflammation and increased ceramide content characterize subjects with high liver fat content independent of obesity. Diabetes 2007;56:1960–1968. [PubMed: 17620421]

13. Haus JM, Kashyap SR, Kasumov T, Zhang R, Kelly KR, Defronzo RA, Kirwan JP. Plasma ceramides are elevated in obese subjects with type 2 diabetes and correlate with the severity of insulin resistance. Diabetes 2009;58:337–343. [PubMed: 19008343]

14. Alkhouri N, Dixon LJ, Feldstein AE. Lipotoxicity in nonalcoholic fatty liver disease: not all lipids are created equal. Exp Rev Gastroenterol Hepatology 2009;3:445–451.

15. Preiss JE, Loomis CR, Bell RM, Niedel JE. Quantitative measurement of sn-1,2-diacylglycerols. Methods Enzymol 1987;141:294–300. [PubMed: 3037247]

16. Gorska M, Dobrzyn A, Zendzian-Piotrowska M, Namiot Z. Concentration and composition of free ceramides in human plasma. Horm Metab Res 2002;34:466–468. [PubMed: 12198604]

17. Dobrzyn A, Gorski J. Ceramides and sphingomyelins in skeletal muscles of the rat: content and composition. Effect of prolonged exercise. Am J Physiol Endocrinol Metab 2002;282:E277–285. [PubMed: 11788358]

18. Yano M, Kishida E, Muneyuki Y, Masuzawa Y. Quantitative analysis of ceramide molecular species by high performance liquid chromatography. J Lipid Res 1998;39:2091–2098. [PubMed: 9788256]

19. Tserng KY, Griffin R. Quantitation and molecular species determination of diacylglycerols, phosphatidylcholines, ceramides, and sphingomyelins with gas chromatography. Anal Biochem 2003;323:84–93. [PubMed: 14622962]

20. Dobrzyn A, Knapp M, Gorski J. Effect of acute exercise and training on metabolism of ceramide in the heart muscle of the rat. Acta Phys Scand 2004;181:313–319.

21. Blachnio-Zabielska A, Baranowski M, Zabielski P, Gorski J. Effect of exercise duration on the key pathways of ceramide metabolism in rat skeletal muscles. J Cell Biochem 2008;105:776–784. [PubMed: 18680146]

22. Turinsky J, O'Sullivan DM, Bayly BP. 1,2-Diacylglycerol and ceramide levels in insulin-resistant tissues of the rat in vivo. J Biol Chem 1990;265:16880–16885. [PubMed: 2211599]

23. Yamaguchi M, Miyashita Y, Kumagai Y, Kojo S. Change in liver and plasma ceramides during D-galactosamine-induced acute hepatic injury by LC-MS/MS. Bioorg Med Chem Lett 2004;14:4061–4064. [PubMed: 15225726]

24. Ichi I, Nakahara K, Fujii K, Iida C, Miyashita Y, Kojo S. Increase of ceramide in the liver and plasma after carbon tetrachloride intoxication in the rat. J Nutr Sci Vitamin 2007;53:53–56.

25. Schmelzer K, Fahy E, Subramaniam S, Dennis EA. The lipid maps initiative in lipidomics. Methods Enzymol 2007;432:171–183. [PubMed: 17954217]

26. Sullards MC, Allegood JC, Kelly S, Wang E, Haynes CA, Park H, Chen Y, Merrill AH Jr. Structure-specific, quantitative methods for analysis of sphingolipids by liquid chromatography-tandem mass spectrometry: "inside-out" sphingolipidomics. Methods Enzymol 2007;432:83–115. [PubMed: 17954214]

27. Haynes TA, Duerksen-Hughes PJ, Filippova M, Filippov V, Zhang K. C18 ceramide analysis in mammalian cells employing reversed-phase high-performance liquid chromatography tandem mass spectrometry. Anal Biochem 2008;378:80–86. [PubMed: 18423390]

28. Bligh EA, Dyer WJ. A rapid and simple method for the determination of esterified fatty acids and for total fatty acids in blood. Can J Biochem Physiol 1959;37:911–917. [PubMed: 13671378]

29. Gu M, Kerwin JL, Watts JD, Aebersold R. Ceramide profiling of complex lipid mixtures by electrospray ionization mass spectrometry. Anal Biochem 1997;244:347–356. [PubMed: 9025952]

30. Liebisch G, Drobnik W, Reil M, Trèumbach B, Arnecke R, Olgemèoller B, Roscher A, Schmitz G. Quantitative measurement of different ceramide species from crude cellular extracts by electrospray ionization tandem mass spectrometry (ESI-MS/MS). J Lipid Res 1999;40:1539–1546. [PubMed: 10428992]

31. Bielawski J, Szulc ZM, Hannun YA, Bielawska A. Simultaneous quantitative analysis of bioactive sphingolipids by high-performance liquid chromatography-tandem mass spectrometry. Methods 2006;39:82–91. [PubMed: 16828308]

32. Merrill AH Jr, Sullards MC, Allegood JC, Kelly S, Wang E. Sphingolipidomics: high-throughput, structure-specific, and quantitative analysis of sphingolipids by liquid chromatography tandem mass spectrometry. Methods 2005;36:207–224. [PubMed: 15894491]

33. Ichi I, Nakahara K, Miyashita Y, Hidaka A, Kutsukake S, Inoue K, Maruyama T, Miwa Y, Harada-Shiba M, Tsushima M, Kojo S. Association of ceramides in human plasma with risk factors of atherosclerosis. Lipids 2006;41:859–863. [PubMed: 17152923]
34. Groener JE, Poorthuis BJ, Kuiper S, Hollak CE, Aerts JM. Plasma glucosylceramide and ceramide in type 1 Gaucher disease patients: correlations with disease severity and response to therapeutic intervention. Biochim Biophys Acta 2008;1781:72–78. [PubMed: 18155675]
35. Baranowski M, Blachnio A, Zabielski P, Gorski J. Pioglitazone induces de novo ceramide synthesis in the rat heart. Prostagl Lipid Mediat 2007;83:99–111.
36. Mano N, Oda Y, Yamada K, Asakawa N, Katayama K. Simultaneous quantitative determination method for sphingolipid metabolites by liquid chromatography/ionspray ionization tandem mass spectrometry. Anal Biochem 1997;244:291–300. [PubMed: 9025946]
37. Tani M, Ito M, Igarashi Y. Ceramide/sphingosine/sphingosine 1-phosphate metabolism on the cell surface and in the extracellular space. Cell Signal 2007;19:229–237. [PubMed: 16963225]
38. Lochhead KM, Zager RA. Fluorinated anesthetic exposure “activates” the renal cortical sphingomyelinase cascade. Kidney Int 1998;54:373–381. [PubMed: 9690203]
39. Lightle S, Tosheva R, Lee A, Queen-Baker J, Boyanovsky B, Shedlofsky S, Nikolova-Karakashian M. Elevation of ceramide in serum lipoproteins during acute phase response in humans and mice: role of serine-palmitoyl transferase. Arch Biochem Biophys 2003;419:120–128. [PubMed: 14592455]

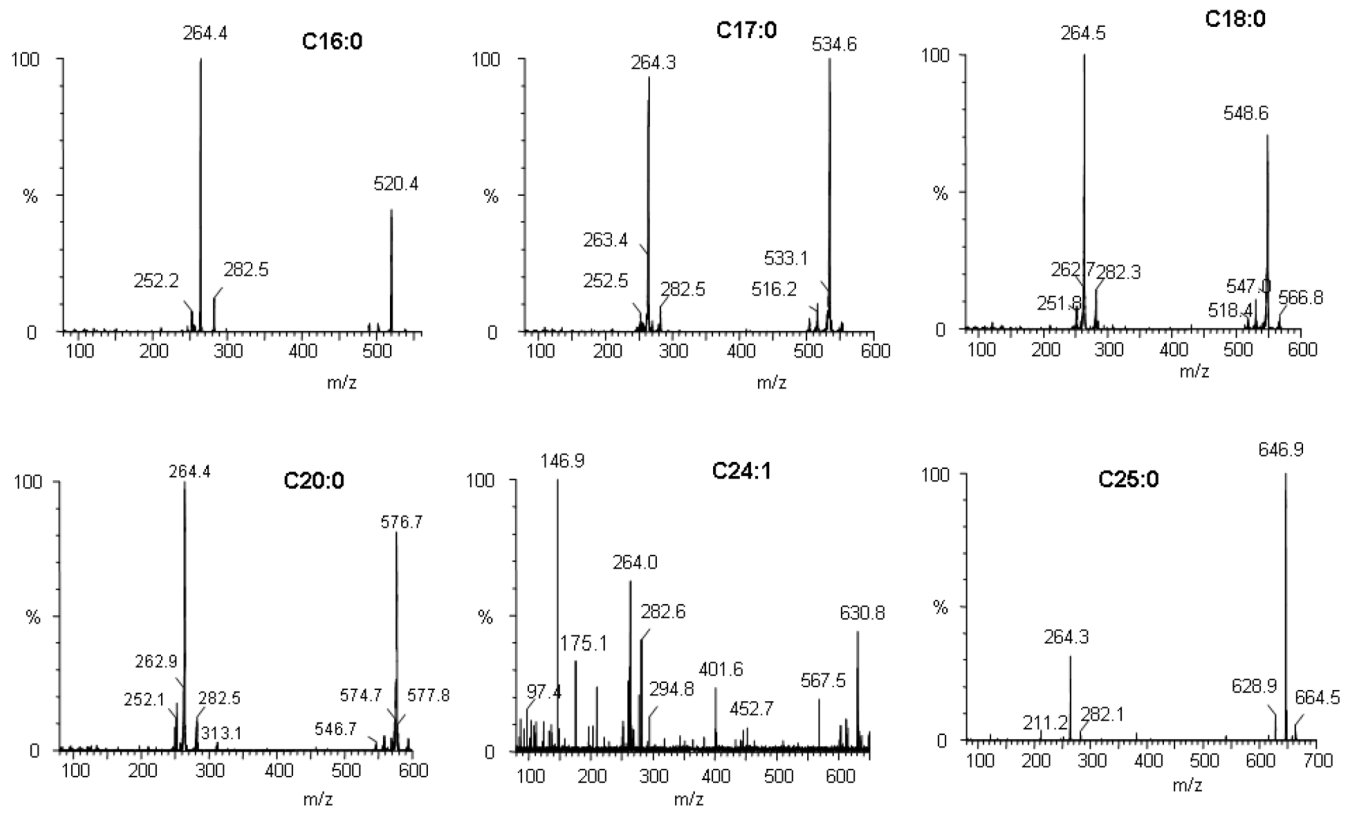

Fig. 1.
Product ions spectra of selected ceramide subspecies in positive ion detection mode.

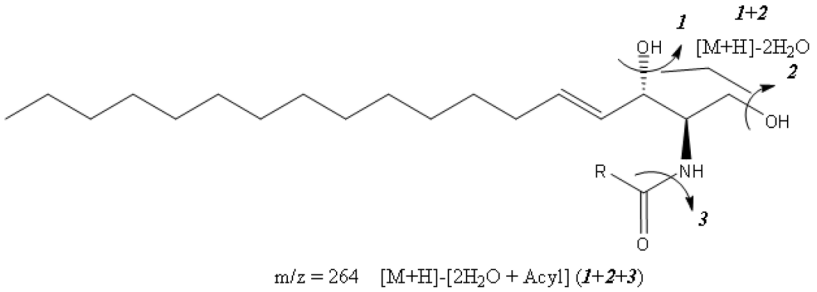

Fig. 2.
Structure and fragmentation pattern of ceramide; m/z 264 is the most abundant product ion during collision induced ionization of ceramides.

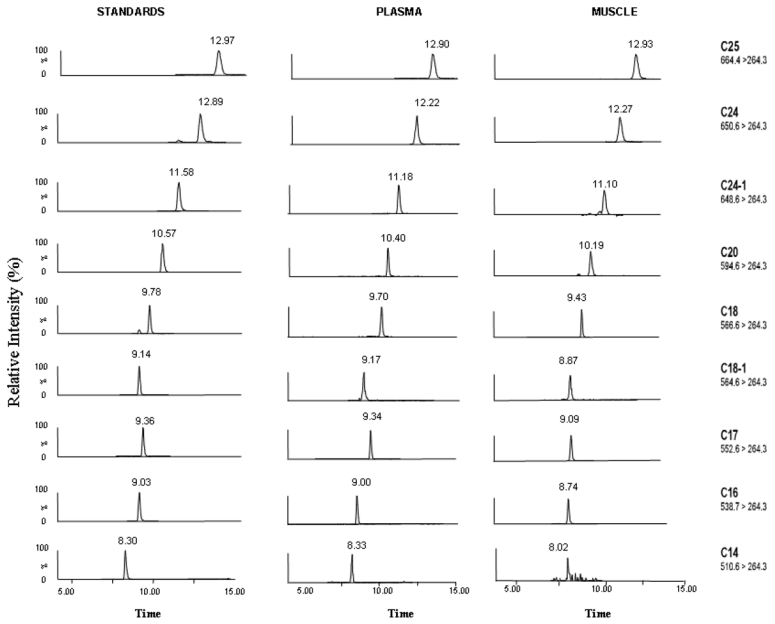

Fig. 3.

Typical chromatograms of standard mixture, plasma, and muscle ceramides, using multiple reaction monitoring mode.

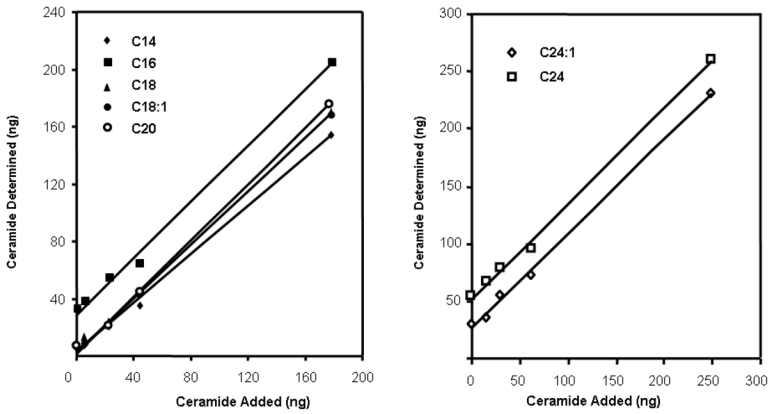

Fig. 4.

Accuracy study for C14, C16, C18, C18:1, C20, C24 and C24:1 ceramides. Known amounts of ceramide species were added to pooled plasma samples (50 μl of each) and the amounts of each ceramide were subsequently quantified. The plot shows ng of ceramide (endogenous plus added) versus ng of ceramide added. The quantification procedure is described in the text.

Table 1

Linearity, analytical sensitivity and detection limit

Ceramide	Limit of Detection (ng/ml)	Limit of Quantification (ng/ml)	Internal Standard	Linear Regression Parameters	
				Slope	r^2
C14	0.005	0.01	C17	0.0239	0.999
C16	0.02	0.05	C17	0.0033	0.998
C18	0.01	0.02	C17	0.0102	0.998
C18:1	0.01	0.02	C17	0.0101	0.996
C20	0.005	0.01	C17	0.0070	0.998
C24	0.05	0.1	C25	0.0113	0.996
C24:1	0.2	0.5	C25	0.0162	0.991

Table 2

Ceramide recovery from plasma. Data from accuracy study presented in Fig. 4 were used for calculation of recovery of ceramide species. The result represents the average of recoveries from plasma at 5 different spiked ceramide concentrations. The calculation procedure is described in the Method's section.

Ceramide	C14	C16	C18	C18:1	C20	C24:1	C24
Recovery (%)	78±7	91±11	83±7	91±10	85±8	79±7	84±5

Table 3

Intra- and interassay variability for ceramide assay in rat liver samples

Ceramide	CV (%)	
	Inter-assay (n = 5)	Intra-assay (n = 5)
C14	0.2	0.2
C16	3.7	2.9
C18	0.9	2.0
C18:1	0.2	0.1
C20	1.4	2.3
C24	3.7	3.3
C24:1	7.3	1.2

Table 4

Ceramide recovery from rat tissues

Tissue Type	Ceramide	Tissue (ng/15 mg w.wt.)	Spike (ng)	Detected Total ng	Recovery (%)
Skeletal Muscle	**C14**	4.5	260.5	217.4	82.1
	C16	41.2	287.0	233.5	71.1
	C18	51.3	627.1	598.7	88.3
	C18:1	4.4	245.7	204.0	81.6
	C20	9.3	429.6	426.0	97.1
	C24	26.1	133.6	150.9	94.5
	C24:1	34.8	155.4	166.2	87.4
Liver Tissue	**C14**	1.9	260.5	213.4	81.3
	C16	287.0	173.5	394.8	85.7
	C18	42.2	627.1	574.6	85.9
	C18:1	2.6	245.7	174.1	70.1
	C20	5.9	429.6	294.8	67.7
	C24	769.3	133.6	786.9	87.2
	C24:1	353.1	155.4	504.8	99.3

Anal Biochem. Author manuscript; available in PMC 2011 June 1.

Table 5

Ceramide content (nmol/g wet weight) in different rat tissues (n=5).

Ceramide	Heart		Liver		Muscle (soleus)	
	Present study	Baranowski M. et al [35]	Present study	Yamaguchi M. et al. [23]	Present study	Dobrzyn A. et al. [17]
C14	4.4±0.1	7.9±1.3	8.9±3.5	-	2.6±0.4	5.7±0.7
C16	33.0±0.9	24.5±5.4	28.7±4.3	34.1±9.2	33.3±8.2	44.9±13.8
C18	19.8±3.8	25.1±5.5	5.5±0.4	7.0±1.9	42.5±3.0	54.6±15.6
C18:1	4.7±0.3	5.5±1.3	2.3±0.7	3.8±0.6	13.1±0.6	24.3±7.2
C20	21.0±3.4	5.2±0.8	4.1±0.9	-	17.2±1.4	-
C24	40.0±2.9	12.3±0.8	119.7±4.7	137.4±30.5	37.1±4.2	-
C24:1	28.0±3.5	-	105.2±13.3	69.8±22.2	29.5±5.0	5.3±1.1
Total	150.7±24.2	101±14.9	314.0±61.7	302.6±51.0	176.1±13.3	161.2±24.8

Table 6

Plasma ceramide levels in healthy adults before and after a 12-week clinical exercise intervention.

Ceramide	Pre-exercise	Post-exercise	P-value
C14	0.26±0.06	0.20±0.09	0.03
C16	1.97±0.73	1.68±0.57	NS
C18	0.73±0.29	0.75±0.12	NS
C18:1	0.06±0.02	0.05±0.02	0.05
C20	0.35±0.07	0.33±0.06	NS
C24	1.48±0.49	0.99±0.25	0.01
C24:1	0.51±0.17	0.39±0.06	NS
Total	5.37±0.55	4.40±0.68	0.01

Data are presented as mean ± SE. All five subjects completed supervised aerobic exercise training: one hour per day, 5 d/wk, at 80% of HRmax (~70% VO2max). Ceramide concentration are expressed in μmol/L.